

## Why do nanowires grow vertically-aligned in the absence of epitaxy

22 September 2018

Almog R. Azulay,<sup>1</sup> Yury Turkulets,<sup>1</sup> Davide Del Gaudio,<sup>2</sup> Rachel S. Goldman,<sup>2</sup> and Ilan Shalish<sup>1\*</sup><sup>1</sup>Ben Gurion University of the Negev, Beer Sheva, Israel <sup>2</sup>University of Michigan at Ann Arbor

Images of uniform and upright nanowires are fascinating, but often, they are quite puzzling, when epitaxial templating from the substrate is clearly absent. Here, we reveal one such hidden growth mechanism through a specific example - the case of ZnO nanowires grown on silicon oxide and glass. We show how electric fields exerted by the insulating substrate may be manipulated through the surface charge to define the orientation of the nanowires. Our results suggest that the growth of wurtzite semiconductors may often be described as a process of electric-charge-induced self assembly.

Several unique features make ZnO one of the most intensively studied semiconductors today.<sup>1</sup> To date, ZnO has been used as a transparent conductor in photovoltaic applications,<sup>2</sup> varistor for voltage surge protection,<sup>3</sup> solar blind photodetector,<sup>4</sup> gas sensor,<sup>5</sup> and photocatalyst material.<sup>6</sup> It has also been proposed for several future applications, as transparent field effect transistors,<sup>7</sup> UV light-emitting diodes,<sup>8</sup> memristors,<sup>9</sup> biosensors,<sup>10</sup> and spintronic devices.<sup>11,12</sup> Growth of ZnO on Si is vital for integrating this material into the present microelectronic technology. One peculiar observation that has become more easily apparent with the growth of ZnO nanowires is that ZnO grows preferentially c-oriented when grown on substrates such as glass and Si that clearly do not provide an epitaxial template.<sup>13</sup> **Figure 1** shows 3 hexagonally shaped ZnO mesas grown on Si(100) substrate. The hexagonal shape confirms that the mesas are indeed c-oriented, i.e., their growth direction is along the *c* axis. The sides of the different hexagonal mesas are clearly not mutually parallel. This confirms the lack of epitaxial relations with the substrate. Growth of c-oriented nanowires on Si substrate, as shown in **Fig. 2**, has been reported in several papers. Several groups have grown vertical c-oriented ZnO nanowire arrays on silicon or glass substrates without the use of a preexisting textured thin film. These were synthesized at temperatures ranging from 400 to 600 °C using metal organic vapor phase epitaxy (MOVPE),<sup>14</sup> chemical vapor deposition (CVD),<sup>15</sup> atomic layer deposition (ALD),<sup>16</sup> chemical vapor transport (CVT),<sup>17</sup> or hydrothermal approach.<sup>18,19</sup> In an attempt to explain the upright alignment, it was suggested that formation of a wetting layer of ZnO, to which the ZnO nanowires could then align epitaxially, could be

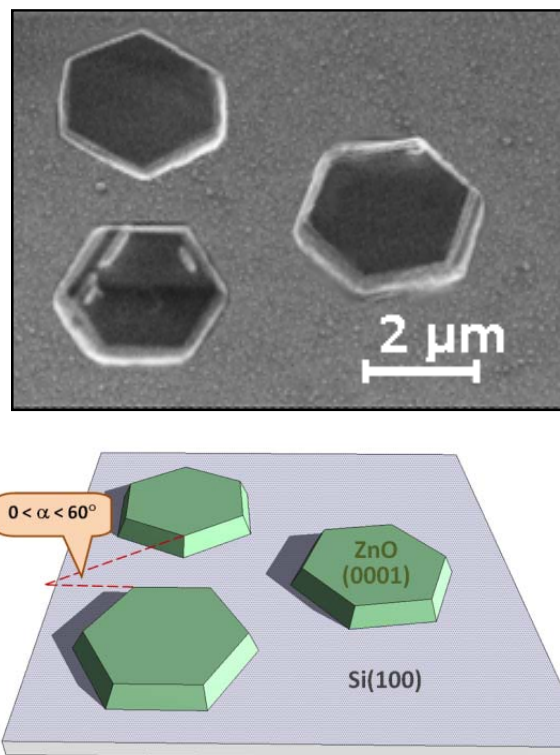


**Figure 1** - SEM image acquired at sample-tilt of 30° of hexagonally shaped mesas grown on Si(100) substrate (top), and schematic cartoon showing the rotational angle difference, which confirms the lack of epitaxial relations with the substrate, despite the alignment of the *c*-axis perpendicular to the substrate.

the cause, but an explanation about why the wetting layer would

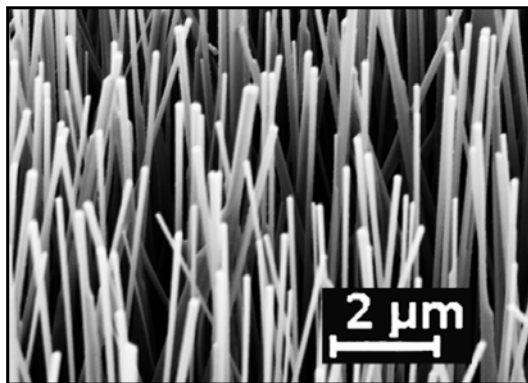


**Figure 2** - SEM image of c-oriented ZnO nanowires grown on Si(100) substrate.

grow c-oriented was not given.<sup>17</sup> An approach employing a similar mechanism was suggested by the group of Peidong Yang.<sup>19</sup> They used zinc acetate spin-coated on the growth substrate. The thermal decomposition of the zinc acetate was suggested to have created ZnO colloids and nanocrystals having their (0002) planes parallel to the substrate surface, but no explanation was offered for this directional alignment of the seed layer. Clearly, the method creates oriented nuclei, from which oriented ZnO nanorods could grow epitaxially on a non-epitaxy substrate. However, the question why the nuclei prefer a specific orientation has remained open.

In contrast to the reported experimental work, several theoretical papers have addressed the problem of the observed oriented growth along the c-axis in attempts to reconcile it with the inherent instability of the polar faces.<sup>20,21,22,23,24</sup> Claeysens et al. suggested a graphitic structure reconstruction of the ZnO of films thinner than 18 monolayers, over which c-oriented growth should be favored.<sup>21</sup> This reconstruction was required in order to cancel the polarization charge present on the polar faces to allow the ZnO to grow on a substrate that was not charged. As a matter of fact, in all of these theoretical studies, no specific substrate was clearly considered as part of the problem. Here, we propose a simple mechanism that resolves the instability problem of the polar faces and renders the reconstruction redundant, at least when the substrate is Si, though the same effect may not be limited to ZnO on Si.

During vapor growth of ZnO, oxygen is an important part of the ambient. At the typically high growth temperatures, the Si substrate will oxidize faster than Zn, due to the lower free energy of formation of SiO<sub>2</sub> (~-727 KJ/mole at 1000 °K) compared with that of ZnO (~-

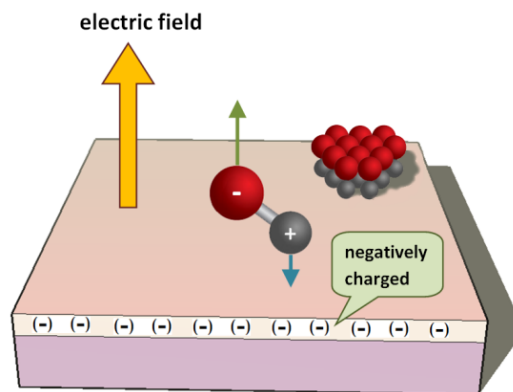


**Figure 3** - Schematic of Si substrate with negatively charged surface oxide, which exerts an electric field that aligns the polar axis of the deposited molecule along electric field lines. For ZnO, the zinc (oxygen) face is positively (negatively) charged; thus the oxygen face points up.

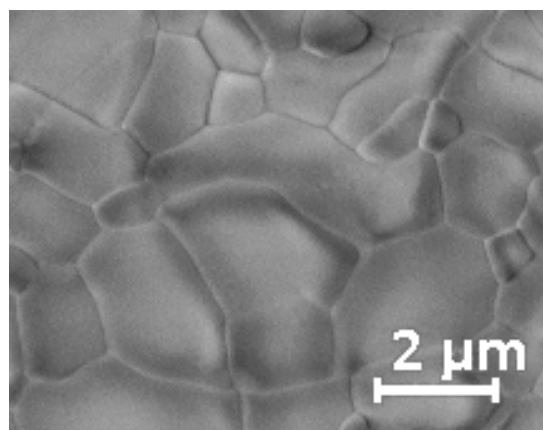


**Figure 4** - Polycrystalline ZnO film grown on a Si(100) substrate. Each individual grain is c-aligned but is rotated on the c-axis in a random angle. When they expand, they meet each other forming grain boundaries.

256 KJ/mole at 1000 °K).<sup>25</sup> As a result, SiO<sub>2</sub> will form immediately at the very early stages of the growth process. The presence of oxygen at the high growth temperature is also known to induce charging in the oxide layer. Charging of the oxide during its growth has been reported already in the early days of the field effect transistor<sup>26</sup> and is a known by-product of the oxide growth process.<sup>27,28,29</sup> Typically, a positive charge is induced during CVD or thermal growth, but may turn negative in plasma enhanced CVD.<sup>30</sup>

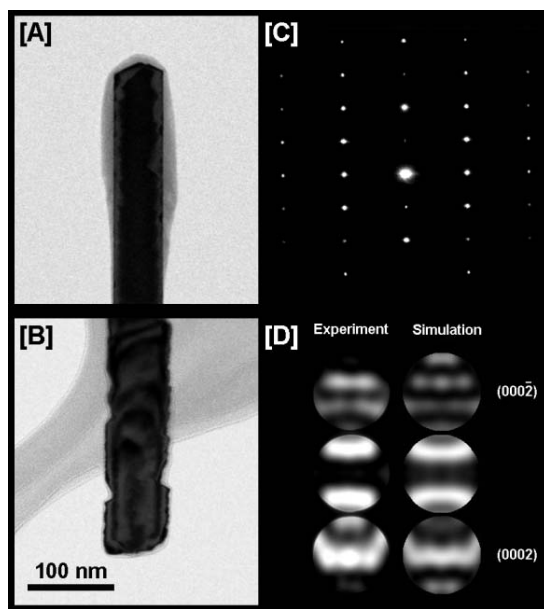


**Figure 5** – [A] TEM of the tip-end of a single CVD-grown ZnO nanowire on thermal oxide (the sample of Fig. 2). [B] TEM image of the bottom/substrate end of the same wire. Note that the bottom of the wire is typically slightly wider with rougher surface. [C] Selective area electron diffraction (SAED), and [D] Experimental and simulated converging beam electron diffraction (CBED) corresponding to the diffraction in [C] acquired from the bottom end of Fig. B. The simulation corresponds to 70-nm-thick ZnO.

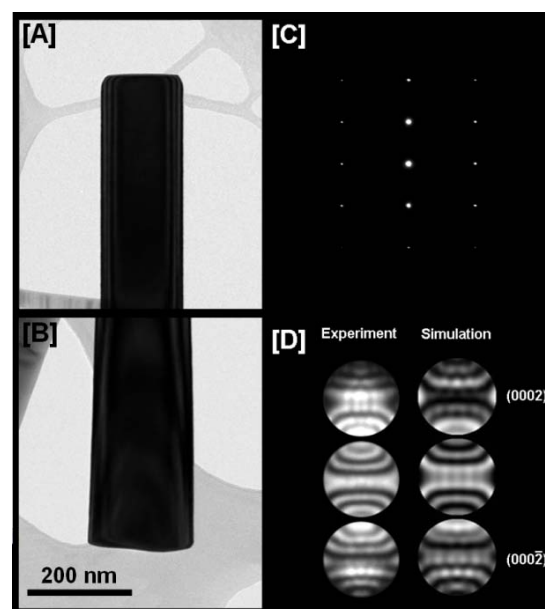


**Figure 6** – [A] TEM of the tip-end of a single CVD-grown ZnO nanowire on PECVD-grown oxide (the sample of Fig. 2). [B] TEM image of the bottom/substrate end of the same wire. [C] Selective area electron diffraction (SAED) shows that the wire is oriented along the  $c$ -axis, and [D] Experimental and simulated converging beam electron diffraction (CBED) corresponding to the diffraction in [C] acquired from the bottom end of Fig. B. The simulation corresponds to 170-nm-thick ZnO (the diffraction was taken slightly off the center of the wire).

As schematically depicted in [Fig. 3](#), this surface charge induces an electric field perpendicular to the substrate surface. As ZnO is a polar material, wherein the polar charge on the oxygen face is negative, the presence of an electric field should work to align the growth perpendicular to the substrate. Hence, a  $c$ -oriented growth is a reasonable outcome.

Since there are no epitaxial relations with the substrate, different individual nuclei may all have their  $c$ -axis perpendicular to the substrate but otherwise are randomly rotated in respect to one another. As the nuclei expand laterally they meet one another forming a polycrystalline film, as in [Fig. 4](#), wherein all the individual crystals may be  $c$ -oriented. Nanowire growth on such a substrate will result in upright nanowires. However, nanowires on different grains will have a random difference in their angle of rotation around their growth axis, reflecting the rotational angle of the grain on which they grew.

If the proposed model is correct, and  $c$ -orientation of the ZnO growth on  $\text{SiO}_2$  is indeed caused by the oxide electric charge, control

of the charge sign may cause (0002) growth in the case of negative charge (electron trapping), in contrast to the commonly observed (000-2) growth on the typical hole-trapping (positively charged) thermally-grown  $\text{SiO}_2$ . To test this experimentally, we grew ZnO nanowires on two different substrates: thermally-grown  $\text{SiO}_2$ , and plasma-enhanced CVD grown  $\text{SiO}_2$ . The presence of negative surface charge was verified using a Kelvin probe.

[Figures 5a](#) and [5b](#) show transmission electron microscopy (TEM) images of the two ends of a CVD-grown ZnO nanowire grown on a *positively* charged thermal oxide. Diffractions were acquired at both ends of each wire to verify that no polarity inversion has taken place during the growth. The shown diffractions were obtained from the bottom/substrate end of the wire shown in [Fig 5b](#). The bottom part of the wire shown in [Fig. 5b](#) is slightly thicker than the other end of the wire – a typical and common observation in nanowires that is useful for identification of the bottom end, especially in cases of self-catalyzed growth which typically lack the catalyst ball at the tip. [Figure 5c](#) shows the selective-area electron diffraction (SAED) pattern acquired from the bottom end of the wire, and [Fig. 5d](#) shows

the corresponding convergent-beam electron diffraction (CBED) pattern side by side with the simulated CBED pattern revealing a (000-2)-oriented growth direction confirming the prediction of our model.

**Figures 6** follows the same structure as Fig. 5 showing TEM and CBED results for a CVD-grown ZnO nanowire grown on a *negatively* charged PECVD oxide. Comparison of the CBED pattern with simulated pattern reveals a (0002)-oriented growth direction confirming the prediction of our model for this case as well.

Based on these CBED results we conclude that substrate charge plays a pivotal role in directing the growth of polar materials, especially polar oxides, such as ZnO, on insulating substrates, such as SiO<sub>2</sub>. Charge induced during the growth of the insulating oxide substrate exerts an electric field that works to align the polar axis of the nucleating nanowire material, working as an unintentional, naturally occurring, electrophoresis on the deposited polar material. To facilitate the polar alignment, it seems necessary to grow the nanowires in a two step process. In the first step, or the nucleation step, it is necessary to limit the amount of the nucleating material, to enable the formation of a seed layer wherein the seeds are aligned. In the second step, epitaxial growth of nanowires may take place on the seed layer. If the first step is bypassed, the high nanowire growth rate typically disturbs the alignment. The small quantity of Zn that is made available for nucleation when using the Zn-acetate method is small enough to allow optimal alignment of the particles that may then serve as seeds for epitaxial growth of ZnO nanowires. The proposed mechanism may not be limited to the ZnO/Si system.

## Experimental Details

High-resistivity (~2000 Ohm-cm) boron-doped 2 inch diameter 280 μm thick single-side polished Si(100) wafers were used as substrates. Charge in the oxide was verified using a Kelvin probe (Besoke Delta PHI GmbH, Germany).<sup>31</sup> The substrates were first deposited with Zn-acetate and annealed to 1020 °C for 30 min to form a seed layer of ZnO. ZnO nanowires were grown in a tube furnace at ~1020 °C under flow of Ar/O<sub>2</sub> of 30/4 sccm. The samples were introduced into the furnace in a quartz crucible containing a mixture of 1:1 ZnO powder and graphite. They were introduced using a linear-motion feed-through after the furnace had reached the desired temperature, and were removed after 5 minutes. TEM imaging and electron diffraction were carried out in a JEOL JEM-2100F instrument operating at 200 kV. CBED simulation was

carried out using Pierre Stadelmann's JEMS electron microscopy simulation software.<sup>32</sup>

## Supplementary Information

Additional TEM/CBED images from several different wires is provided for each of the two oxide types used in the experiment.

## Acknowledgement

This work was funded by NSF/BSF EECS (BSF grant #2015700).

## References

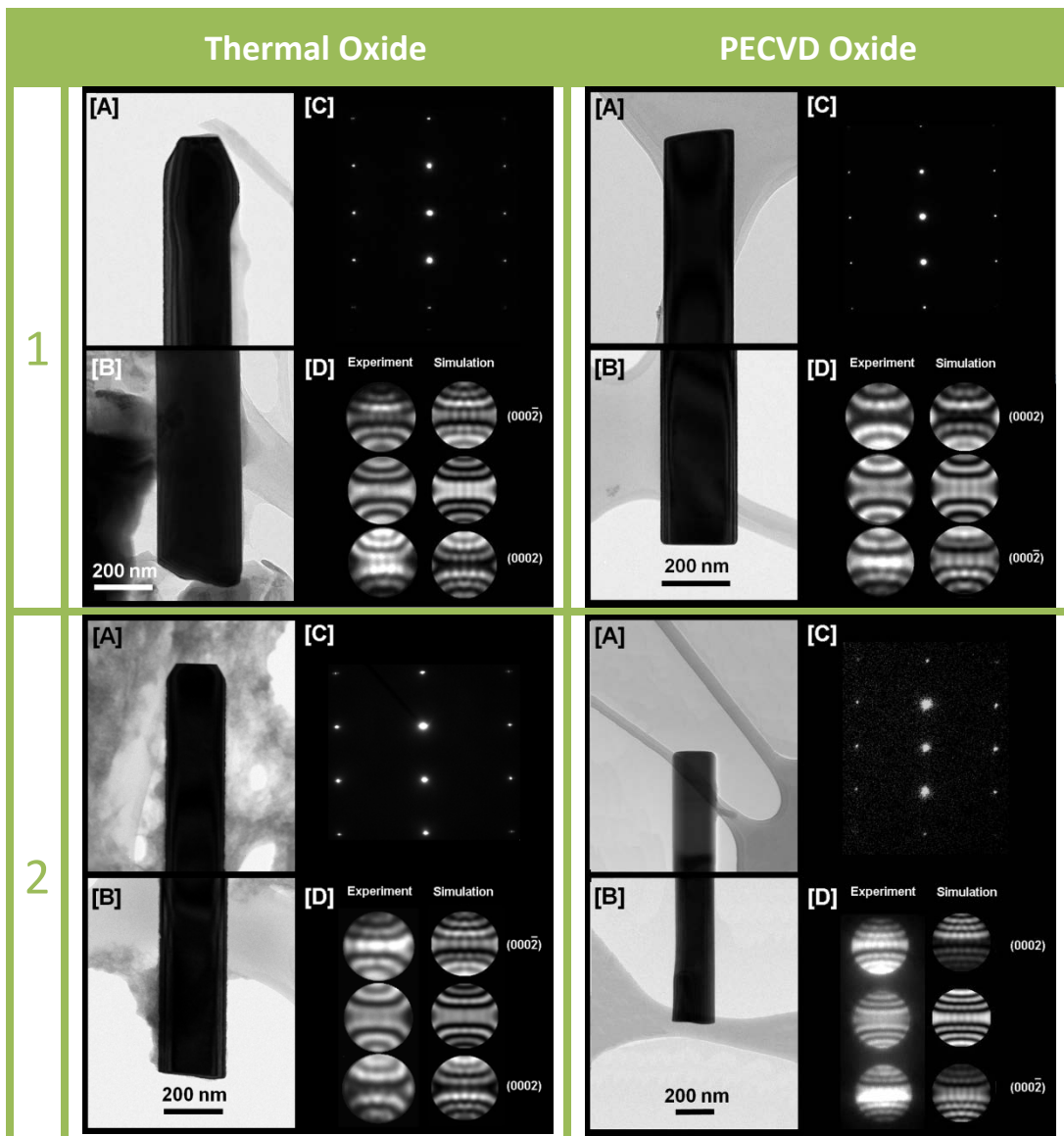
- <sup>1</sup> Ü. Özgür, Ya. I. Alivov, C. Liu, A. Teke, M.A. Reshchikov, S. Doğan, Vitaliy Avrutin, S.-J. Cho, H. Morkoç. A comprehensive review of ZnO materials and devices. *J. Appl. Phys.* **98**, 041301 (2005). DOI: 10.1063/1.1992666
- <sup>2</sup> A. Polman, M. Knight, E.C. Garnett, B. Ehrler, W.C. Sinke. Photovoltaic materials: Present efficiencies and future challenges. *Science* **352**, 307 (2016). DOI: 10.1126/science.aad4424
- <sup>3</sup> H. Zhao, J. Hu, S. Chen, Q. Xie, J. He. High nonlinearity and high voltage gradient ZnO varistor ceramics tailored by combining Ga<sub>2</sub>O<sub>3</sub>, Al<sub>2</sub>O<sub>3</sub>, and Y<sub>2</sub>O<sub>3</sub> dopants. *J. Am. Ceram. Soc.* **99**, 769 (2016). DOI: 10.1111/jace.14110
- <sup>4</sup> M.R. Alenezi, S.J. Henley, S.R.P. Silva. On-chip Fabrication of High Performance Nanostructured ZnO UV Detectors. *Sci. Rep.* **5**, 8516 (2015). DOI: 10.1038/srep08516
- <sup>5</sup> M. Drobek, J.-H. Kim, M. Bechelany, C. Vallicari, A. Julbe, and S.S. Kim. MOF-Based Membrane Encapsulated ZnO Nanowires for Enhanced Gas Sensor Selectivity. *ACS Appl. Mater. Interfaces*, **8**, 8323 (2016). DOI: 10.1021/acsami.5b12062
- <sup>6</sup> C.B. Onga, L. Y. Ngb, A.W. Mohammad. A review of ZnO nanoparticles as solar photocatalysts: Synthesis, mechanisms and applications. *Ren. Sustain. Ener. Rev.* **81**, 536 (2018). DOI: 10.1016/j.rser.2017.08.020
- <sup>7</sup> C.-C. Shih, W.-Y. Lee, Y.-C. Chiu, H.-W. Hsu, H.-C. Chang, C.-L. Liu, W.-C. Chen. High performance transparent transistor memory devices using nano-floating gate of polymer/ZnO nanocomposites. *Sci. Rep.* **6**, 20129 (2016). DOI: 10.1038/srep20129
- <sup>8</sup> J. Lu, Z. Shi, Y. Wang, Y. Lin, Q. Zhu, Z. Tian, J. Dai, S. Wang, C. Xu. Plasmon-enhanced Electrically Light-emitting from ZnO Nanorod Arrays/p-GaN Heterostructure Devices. *Sci. Rep.* **6**, 25645 (2016). DOI: 10.1038/srep25645
- <sup>9</sup> B. Kerr Barnes, K.S. Das. Resistance Switching and Memristive Hysteresis in Visible-Light-Activated Adsorbed ZnO Thin Films. *Sci. Rep.*, **8**, 2184 (2018). DOI: 10.1038/s41598-018-20598-5
- <sup>10</sup> H.A. Wahab, A.A. Salama, A.A. El Saied, M. Willander, O. Nur, I.K. Battisha. Zinc Oxide nano-rods based glucose biosensor devices fabrication. *Results in Physics* **9**, 809 (2018). DOI: 10.1016/j.rinp.2018.02.077
- <sup>11</sup> L. Zhu, Y. Zhang, P. Lin, Y. Wang, L. Yang, L. Chen, L. Wang, B. Chen, Z.L. Wang. Piezotronic Effect on Rashba Spin-Orbit Coupling in a ZnO/P3HT Nanowire Array Structure. *ACS Nano*, **12**, 1811 (2018). DOI: 10.1021/acsnano.7b08618
- <sup>12</sup> M. Aras, Ç. Kılıç. Electrical tuning of spin splitting in Bi-doped ZnO nanowires. *Phys. Rev. B* **97**, 035405 (2018). DOI: 10.1103/PhysRevB.97.035405
- <sup>13</sup> Q. Zhou, J.Z. Wen, P. Zhao, W.A. Anderson. Synthesis of vertically-aligned zinc oxide nanowires and their application as a photocatalyst. *Nanomaterials* **7**, 9 (2017). DOI:10.3390/nano7010009
- <sup>14</sup> W. Park, D.H. Kim, S. Jung, G.-C. Yi. Metalorganic vapor-phase epitaxial growth of vertically well-aligned ZnO nanorods. *Appl. Phys. Lett.*, **80**, 4232 (2002). DOI: 10.1063/1.1482800
- <sup>15</sup> J. Wu, S.C. Liu. Low-Temperature Growth of Well-Aligned ZnO Nanorods by Chemical Vapor Deposition. *Adv. Mater.* **14**, 215 (2002). DOI: 10.1002/1521-4095(20020205)14:3<215::AID-ADMA215>3.0.CO;2-J
- <sup>16</sup> Q. Li, V. Kumar, Y. Li, H. Zhang, T.J. Marks, R.P.H. Chang. Fabrication of ZnO Nanorods and Nanotubes in Aqueous Solutions. *Chem. Mater.*, **17**, 1001-1006 (2005). DOI: 10.1021/cm048144q
- <sup>17</sup> H. Zhang, X. Sun, R. Wang, D. Yu. Growth and formation mechanism of c-oriented ZnO nanorod arrays deposited on glass. *Cryst. Growth*, **269**, 464 (2004). DOI: 10.1016/j.jcrysgro.2004.05.078
- <sup>18</sup> T. Ma, M. Guo, M. Zhang, Y. Zhang, X. Wang. Density controlled hydrothermal growth of well aligned ZnO nanorods arrays. *Nanotechnology* **18**, 035605 (2007). DOI: 10.1088/0957-4484/18/3/035605
- <sup>19</sup> L.E. Greene, M. Law, D.H. Tan, M. Motano, J. Goldberger, G. Somorjai, P.D. Yang. General Route to vertical ZnO Nanowire Arrays Using Textured ZnO Seeds. *Nano Lett.* **5**, 7, 1231 (2005). DOI: 10.1021/nl050788p
- <sup>20</sup> A. Wander, F. Schedin, P. Steadman, A. Norris, R. McGrath, T.S. Turner, G. Thornton, N.M. Harrison. Stability of Polar Oxide Surfaces. *Phys. Rev. Lett.* **86**, 3811 (2001). DOI: 10.1103/PhysRevLett.86.3811
- <sup>21</sup> F. Claeysens, C.L. Freeman, N.L. Allan, Y. Sun, M.N.R. Ashfold, J.H. Harding. Growth of ZnO thin films—experiment and theory. *J. Mater. Chem.*, **15**, 139 (2005). DOI: 10.1039/B414111C
- <sup>22</sup> C.L. Freeman, F. Claeysens, N.L. Allan, J.H. Harding. Graphitic Nanofilms as Precursors to Wurtzite Films: Theory. *Phys. Rev. Lett* **96**, 066102 (2006). DOI: 10.1103/PhysRevLett.96.066102
- <sup>23</sup> C. Noguera, J. Goniakowski. Polarity in oxide ultrathin films. *J. Phys.: Condens. Matter* **20**, 264003 (2008). DOI: 10.1088/0953-8984/20/26/264003
- <sup>24</sup> D. Mora-Fonz, T. Lazauskas, M.R. Farrow, C.R.A. Catlow, S.M. Woodley, A.A. Sokol. Why Are Polar Surfaces of ZnO Stable? *Chem. Mater.* **29**, 5306 (2017). DOI: 10.1021/acs.chemmater.7b01487
- <sup>25</sup> W.F. Gale, T.C. Totemeier, Eds. 2004. *Smithells Metals Reference Book, 8th ed.* Amsterdam: Elsevier. ISBN 0 7506 7509 8. p. 8-26
- <sup>26</sup> M.M. Atalla, E. Tannenbaum, E.J. Scheibner. Stabilization of Silicon surfaces by thermally grown oxides. *Bell Sys. Tech. J.* **38**, 749 (1959). DOI: 10.1002%2Fj.1538-7305.1959.tb03907.x
- <sup>27</sup> B.E. Deal, M. Sklar, A.S. Grove, E.H. Snow. Characteristics of the Surface-State Charge of Thermally Oxidized Silicon. *J. Electrochem. Soc.* **114**, 266 (1967). DOI: 10.1149/1.2426565
- <sup>28</sup> B.E. Deal. The Current Understanding of Charges in the Thermally Oxidized Silicon Structure. *J. Electrochem. Soc.* **121**, 198C (1974). DOI: 10.1149/1.2402380
- <sup>29</sup> A. Boogaard, A.Y. Kovalgin, R.A.M. Wolters. Net negative charge in low-temperature SiO<sub>2</sub> gate dielectric layers. *Microelectron. Eng.*, **86**, 1707 (2009). DOI: 10.1016/j.mee.2009.03.124
- <sup>30</sup> A. Boogaard, A.Y. Kovalgin, R.A.M. Wolters. Negative Charge in Plasma Oxidized SiO<sub>2</sub> Layers. *ECS Transactions*, **35**, 259 (2011). DOI: 10.1149/1.3572288
- <sup>31</sup> For details of the technique, see D.K. Schroder. 2006. *Semiconductor Material and Device Characterization, 3rd ed.* New Jersey: Wiley. ISBN: 978-0-471-73906-7. p. 538.
- <sup>32</sup> P. Stadelmann. 2004 JEMS, electron microscopy software, java version. <http://cimewww.epfl.ch/people/stadelmann/jemsWebSite/jems.html>

# Why do nanowires grow vertically-aligned in the absence of epitaxy

Almog R. Azulay, Yury Turkulets, Davide Del Gaudio, Rachel S. Goldman, and Ilan Shalish

## Supplementary Information

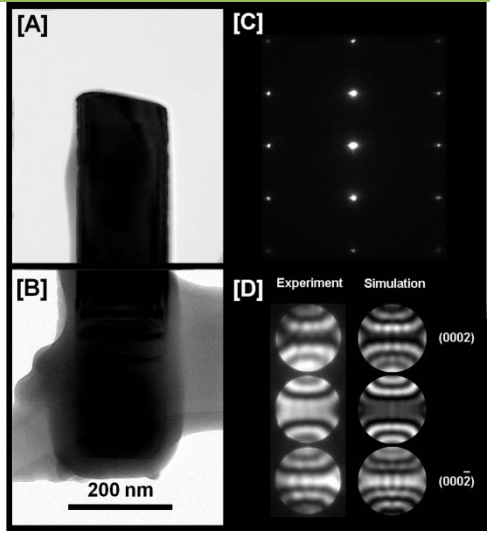
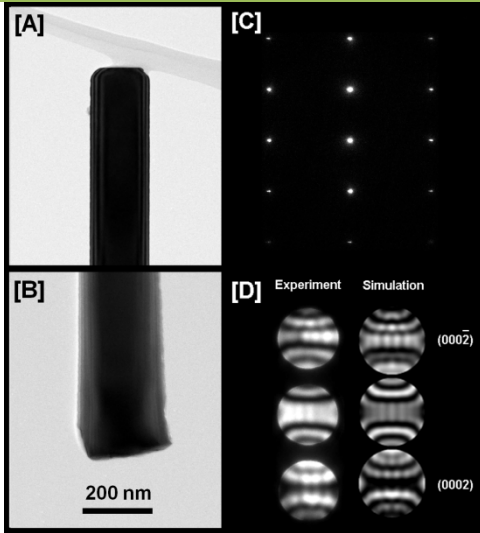
This file contains a table with additional CBED data. In thin wires the CBED pattern is blurred, and this makes it more difficult to compare it to simulation (see e.g. the thermal oxide CBED in line 4 below). For this reason, most of the CBED were acquired from thick wires. For each wire, CBED was acquired from both the bottom and the top of the wire to make sure that the polarity is identical throughout the wire. However for brevity, we show only a single pattern. In each figure, panel A shows the top end of the wire, panel B shows the bottom end, panel C shows the SAED pattern, and panel D compares the CBED pattern with a simulated CBED pattern.



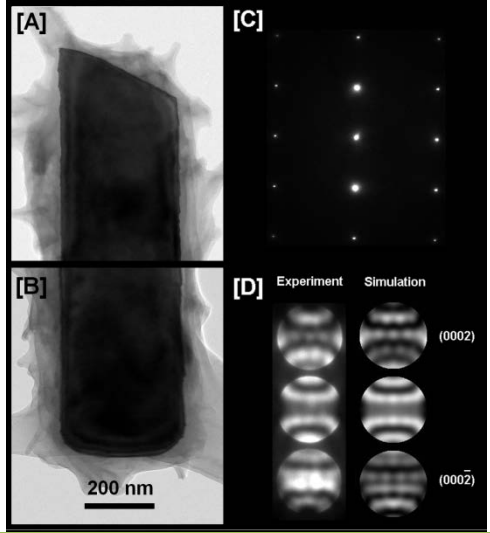
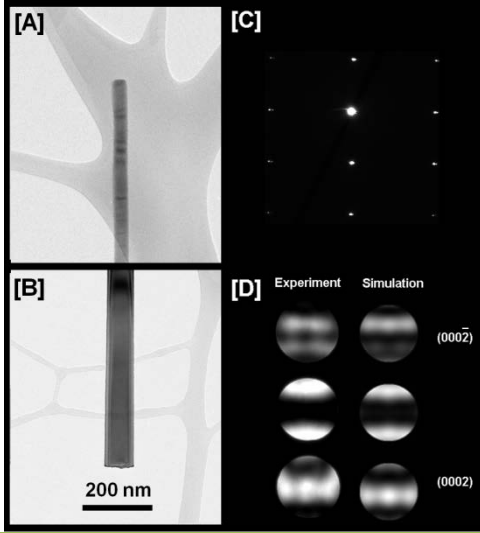
Thermal Oxide

PECVD Oxide

3



4



5

